BEAM PHYSICS AT THE

ADVANCED PHOTON SOURCE

KATHERINE HARKAY

APS, Argonne National Laboratory

CASA Seminar, JLab

January 31, 2003

Accelerator and FEL Physics Group

Katherine Harkay, group leader

John Lewellen, deputy

Yong-chul Chae

Yuelin Li

Vadim Sajaev

Chun-xi Wang

Lee Teng

Acknowledgements, former members

Stephen Milton (now LCLS project head at APS)

Zhirong Huang (now at SLAC)

Eliane Lessner (now at RIA/ANL)

Su-bin Song (former post-doc), Ed Crosbie (retired)

APS Impedance, Instability, Feedback Task Force contributors:

Michael Borland, Louis Emery, Alex Lumpkin,

Ali Nassiri, Nick Sereno, Bingxin Yang, C-Y. Yao

Outline

- Introduction
- Near-term issues
  - o Instabilities
  - o Impedance Database
- Related R&D
  - o Lattice characterization
- Mid- to far-term R&D
- Summary

Basic APS Parameters

Energy [GeV]	7.0
Circumference [m]	1104
RF frequency [MHz]	351.9
RF harmonic no.	1296
Nominal RF voltage [MV]	9.5
Momentum compaction	2.9×10^{-4}
Synchrotron tune	7.0×10^{-3}
Emittance H [nm·rad]	2.4
Coupling [%]	3 %
Nom. chromaticity, ξ[1] H / V	5 / 7
Damping time H/V/L [ms]	9.5 / 9.5 / 4.7

[1] $\xi = \Delta\nu/(\Delta p/p)$

Advanced Photon Source site

25 of 40 sectors are occupied with photon beamlines: bending magnet and insertion device (ID) synchrotron radiation

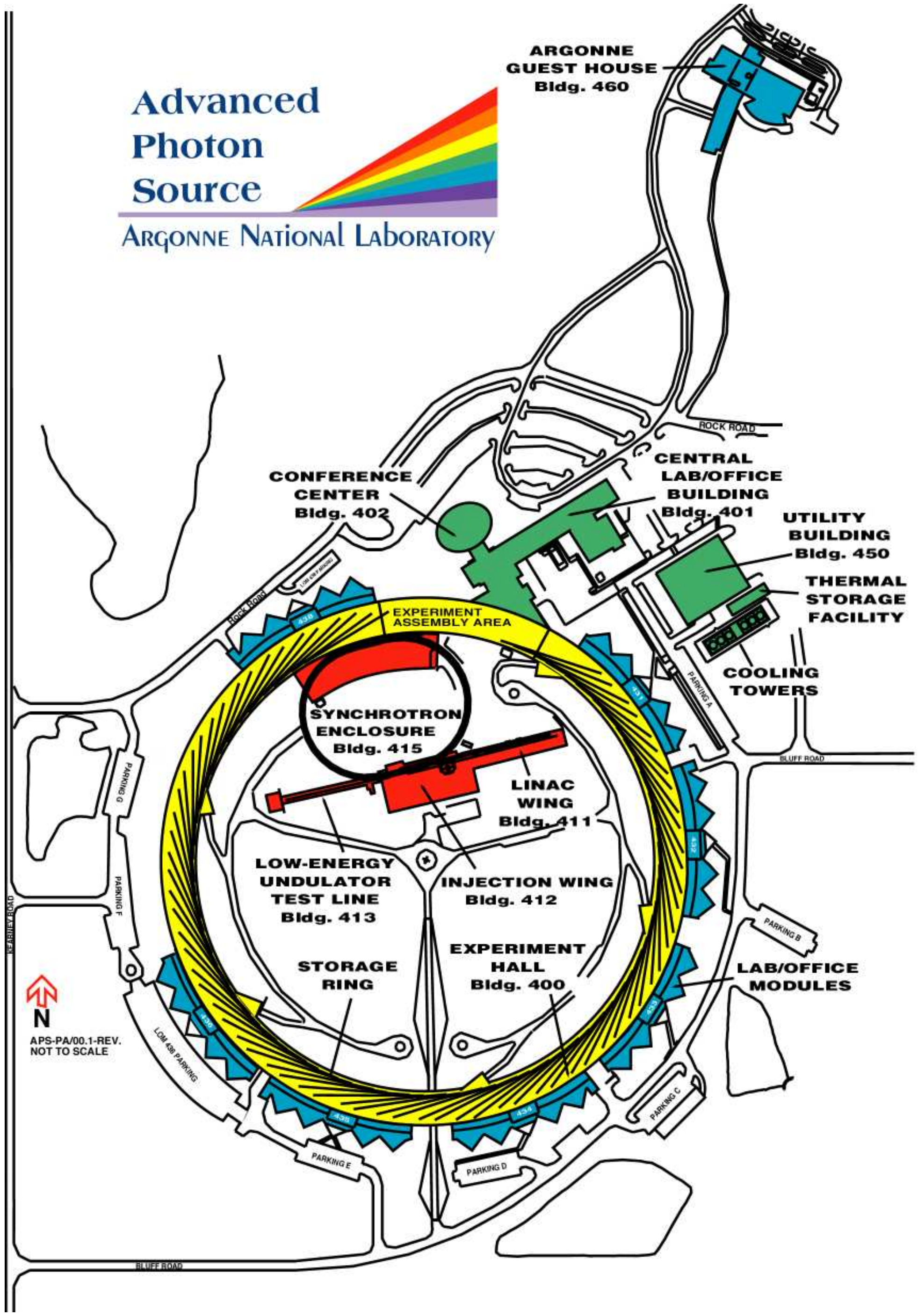

Typical APS storage ring sector

Insertion Device (undulator magnet) with ID chamber

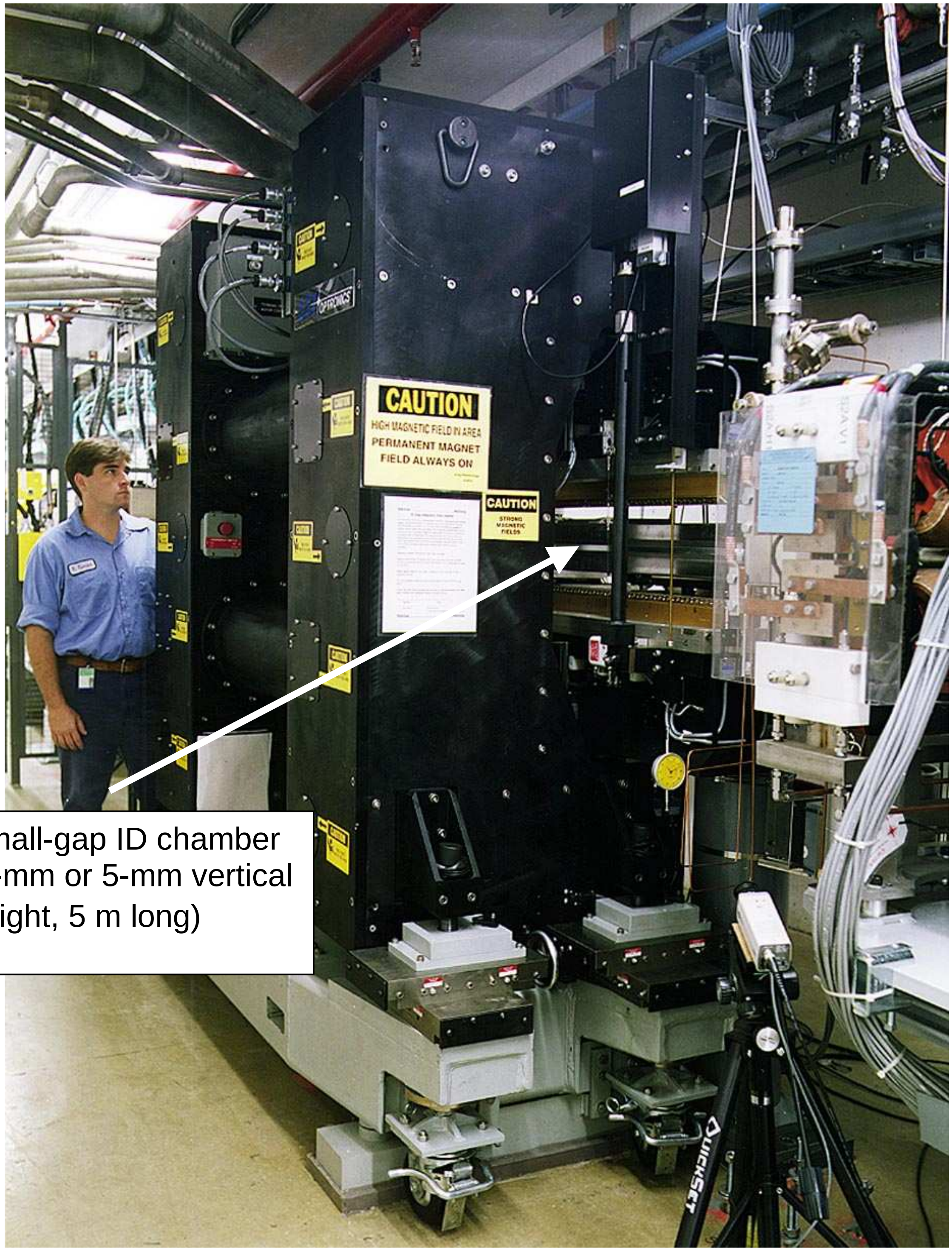

Small-gap ID chamber
(8-mm or 5-mm vertical
height, 5 m long)

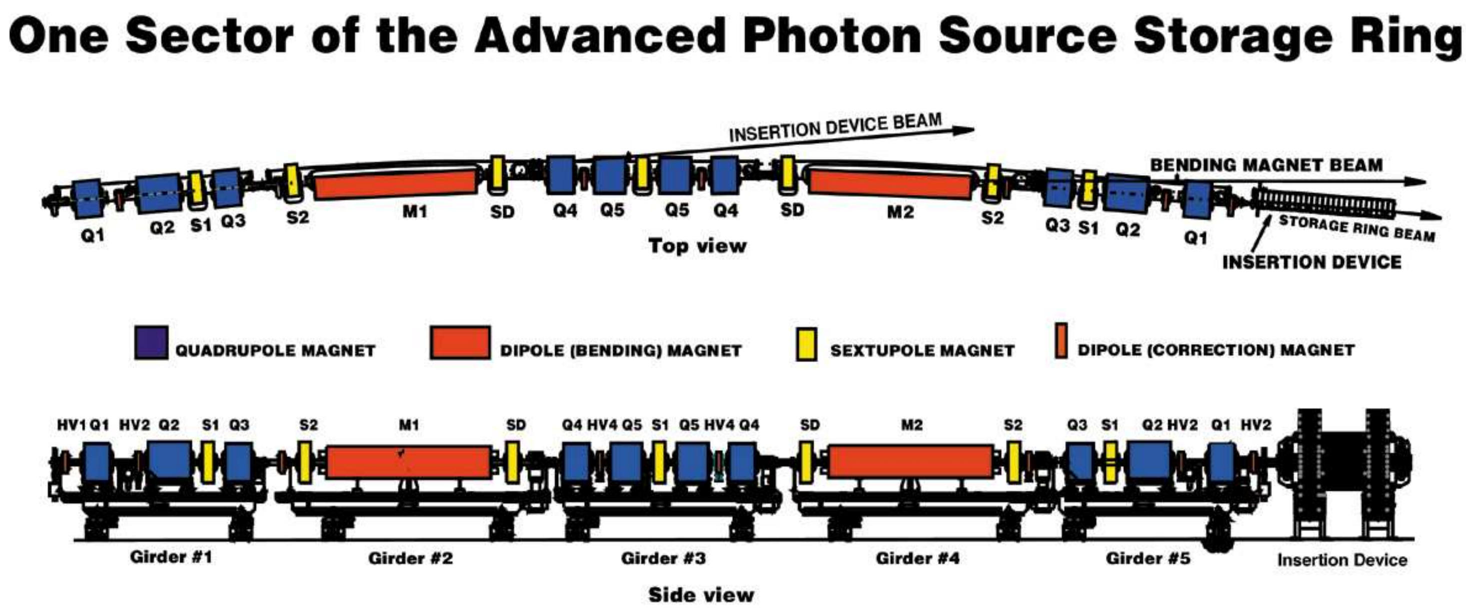

Small-gap ID chambers are located in 5-m straight sections
(total no.: 22 with 8-mm gap, 2 with 5-mm gap, 1 with 19.6-mm gap)

A word on SR User operation

- Standard (~75%) (τ ~ 7-9 h)
  - o 100 mA
  - o Low emittance lattice (2.4 nm-rad)
  - o 23 bunches spaced at h/24 (one missing) (4.3 mA/bunch)
  - o Top-up
- Special operating modes (typ. 1-2 weeks ea. per run)
  - o High emittance, non-top-up (7.7 nm-rad) (τ ~ 20 h)
  - o Hybrid mode (1 or 3 + 56) (τ ~ 20 h)
  - o Many-bunch mode (324 bunches) (τ ~ 100 h)

Near-term Issues

- Typically deliver 100-mA electron beam in 23 bunches (4.3 mA/bunch) for normal operation for users
- Horizontal instability (centroid oscillations) observed above about 5 mA/bunch – this is above the transverse mode-coupling instability (TMCI) threshold
- Normal operation with high positive chromaticity allows a single-bunch intensity limit > TMCI limit: up to about 10 mA. However, beam properties degraded (effective emittance).
- Addition over time of small-gap insertion device chambers, our major source of coupling impedance, has
  - lowered single-bunch instability and intensity limit
  - required operation with higher chromaticity and smaller beta functions to restore
- Need to understand physics and how to control instability in order to
  - satisfy anticipated future user requirement for higher bunch current
  - anticipate effect of additional small-gap insertion device chambers *and influence design*
  - mitigate instability while preserving beam quality, in particular, beam lifetime (e.g., effect of high chromaticity)

Single-bunch instability: transverse mode coupling instability

Force due to transverse wake defocuses beam, i.e., detunes betatron frequency.

When ν_β crosses ($m\nu_s$) modulation sidebands, synchrotron motion can couple to transverse plane and beam can be lost unless chromaticity is sufficiently large/positive.

Tune slope increases with no. of small gap chambers: mode merging threshold decreases.

Horizontal **ξ_x > 1.3, $\xi_y \approx$ 4** **Vertical**

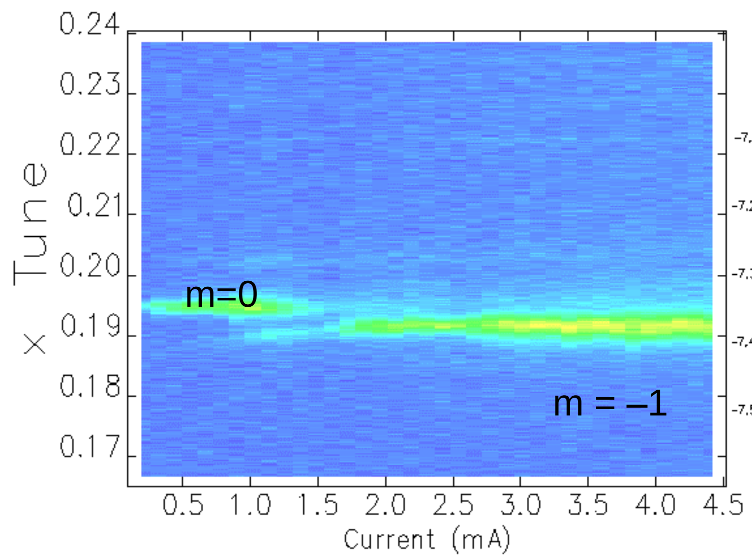

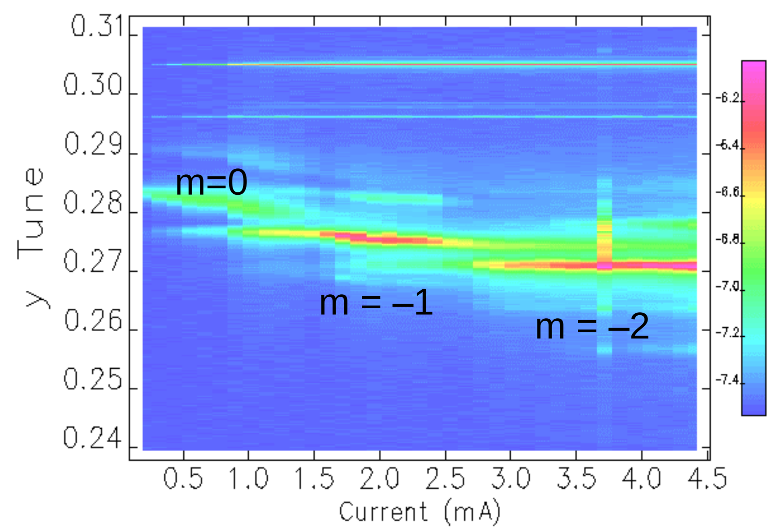

$\Delta\nu_x/\Delta I$ = -8x10^{-4}/mA

$\Delta\nu_y/\Delta I$ = -2.6x10^{-3}/mA

(data courtesy of L. Emery [K. Harkay et al., Proc. of 1999 PAC, 1644])

Transverse Mode-Coupling Instability

(a.k.a. strong head-tail, fast head-tail, transverse turbulence)

from A. Chao, *Physics of Collective Beam Instabilities in High Energy Accelerators*, John Wiley & Sons (1993):

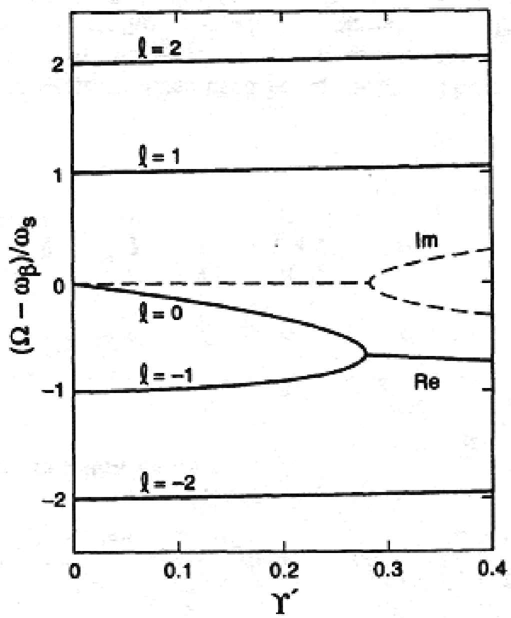

Figure 6.36. Transverse mode frequencies $(\Omega - \omega_\beta)/\omega_s$ versus the parameter Υ' for an air-bag beam with the impedance (6.224). The instability threshold is located at $\Upsilon'_{th} \approx 0.28$, where the modes $l = 0$ and -1 become degenerate. The dashed curves give the imaginary part of the mode frequencies for $l = 0$ and $l = -1$.

BB: $$Z_1^{\perp}(\omega) = \frac{2c}{b^2\omega_0} R_0 \left|\frac{\omega_0}{\omega}\right|^{3/2} [\mathrm{sgn}(\omega) - j]$$

$$\Upsilon' = \frac{N r_0 c^2 R_0}{\gamma T_0 \omega_\beta \omega_s b^2} \sqrt{\frac{\hat{z}}{c T_0}}$$

Tune slope, $\Delta\nu/\Delta I$, from transverse reactive wake:

$$\frac{\Delta\nu}{\Delta I} \propto \frac{\nu_0}{\sigma_z} \frac{\langle\beta\rangle R}{E/e} \overline{Z}_{\perp}(\omega)$$

where R = ring radius, $\overline{Z}_{\perp}(\omega)$ = effective impedance

Two instability modes observed above TBCI; not observed in any other ring with $\xi > 0$

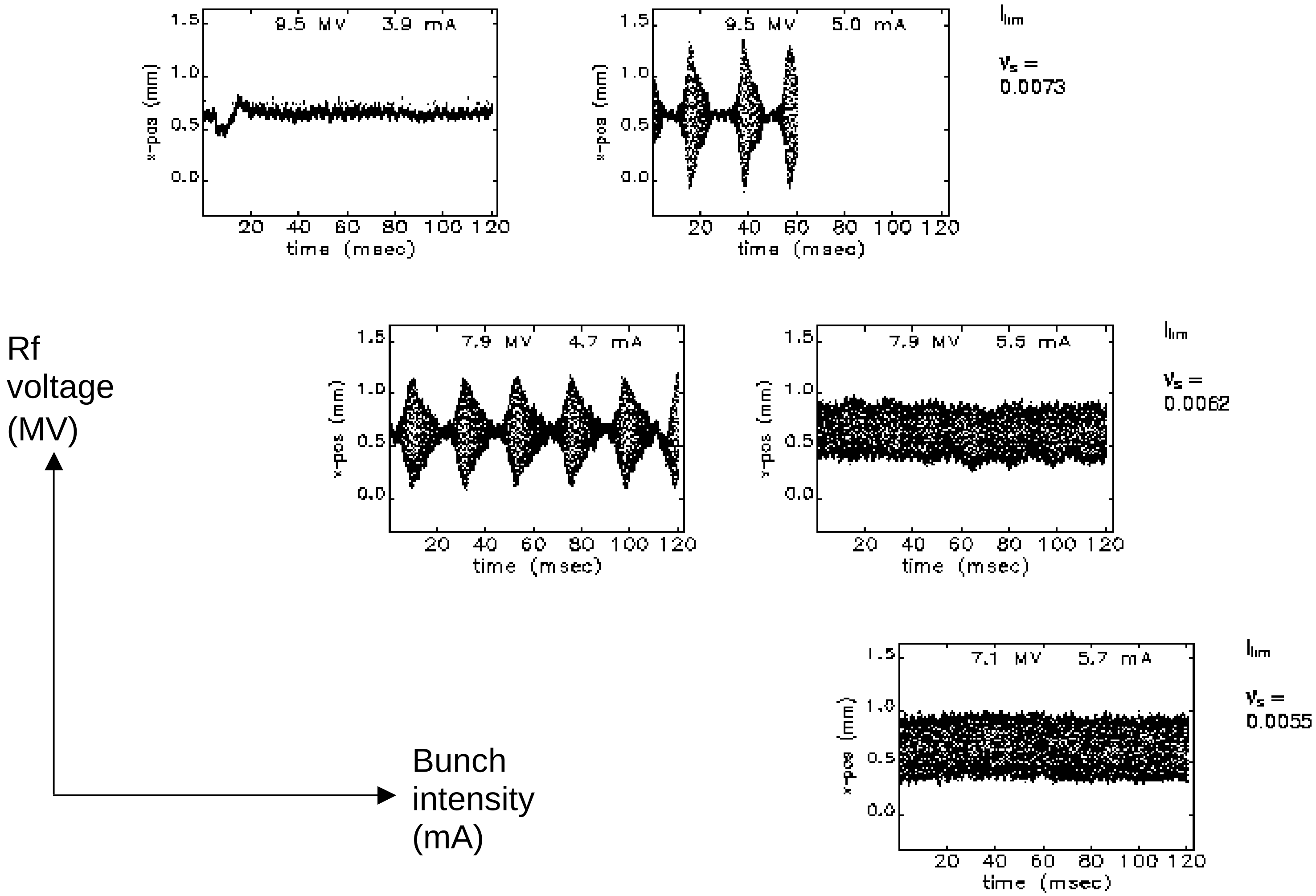

Early APS data using beam position monitor turn-by-turn histories showed horizontal centroid oscillations whose bunch intensity instability onset and mode (bursting vs. steady-state amplitude) varied with rf voltage (chromaticities: ξ_x = 1.3, ξ_y = 3.9) (2/15/1999)

Large <x> oscillations above mode-merging threshold (V_{rf} 9.4 MV case shown): some Users will observe an effective emittance blowup, $\Delta\varepsilon_x$

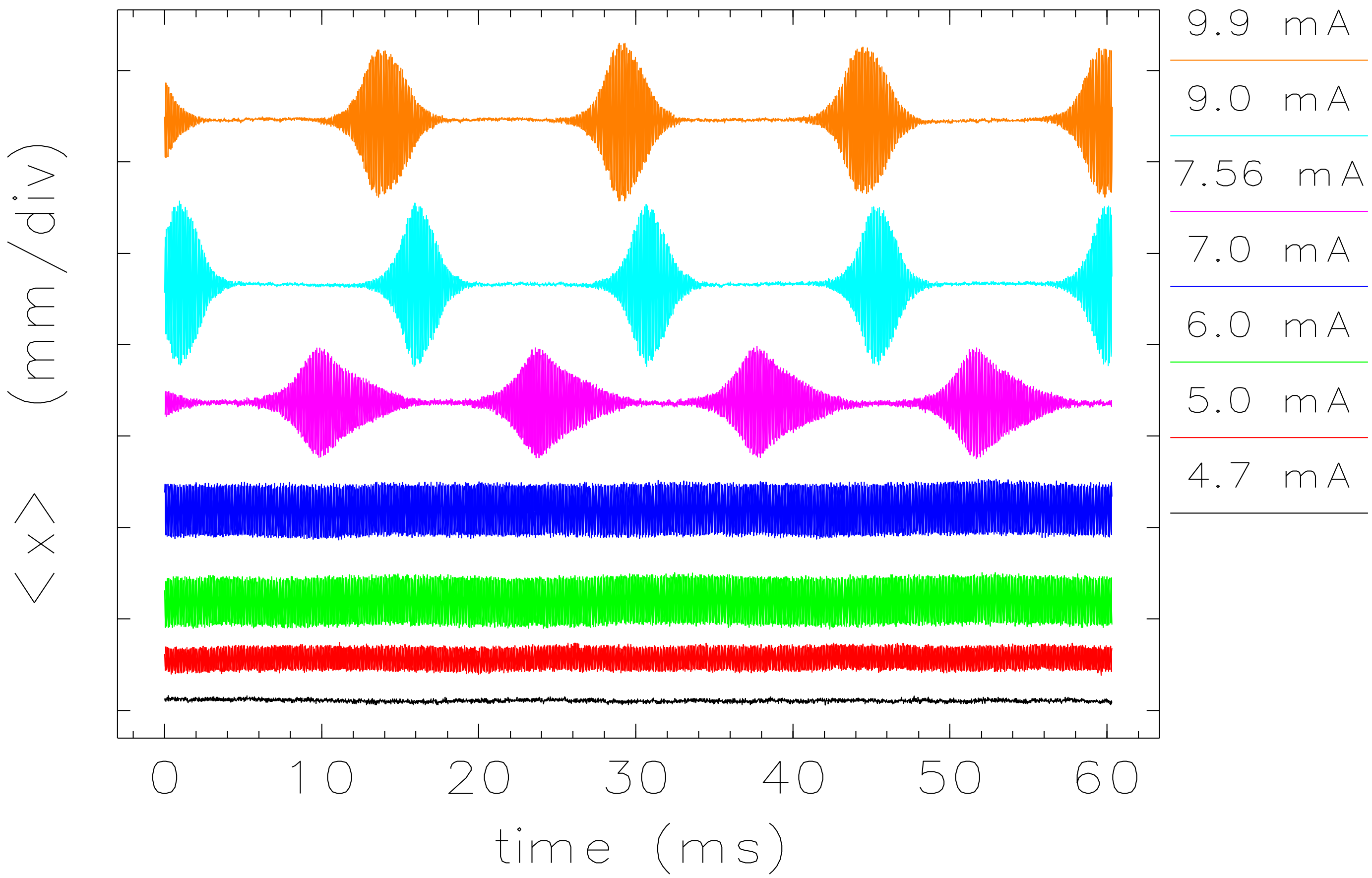

Note: bunch length σ_z, energy spread δ, and emittance ε_x also vary with current

(ε_x decoherence NOT 100% of <x> oscillation amplitude; σ_x = 220 μm (7.5 nm-r lattice))

Variations with different machine parameters

7.5 nm lattice, Vrf = 7.3 MV, $\xi_{x,y}$ = (3,6)

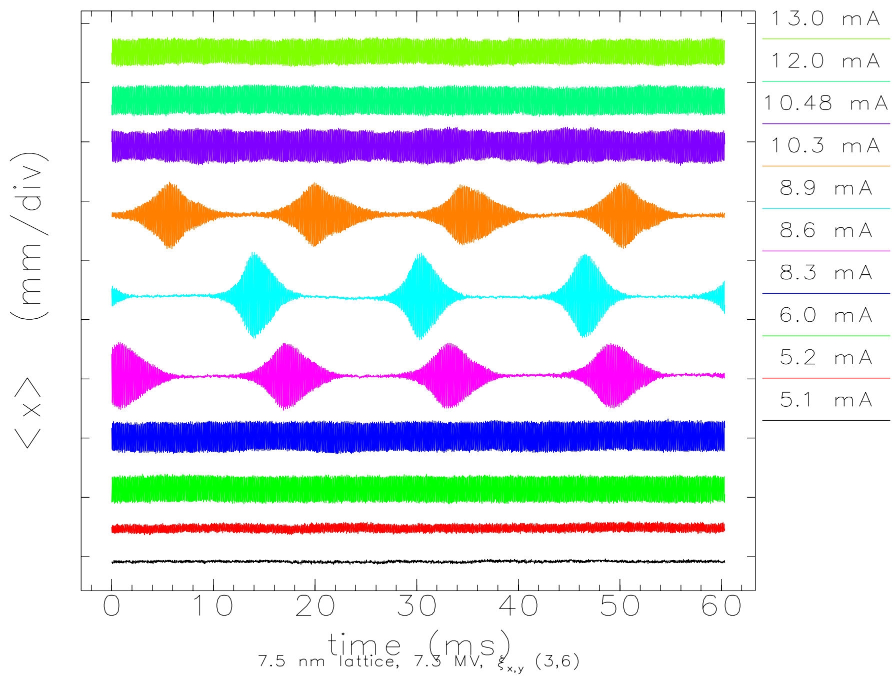

Peak-to-peak amplitude as a function of Vrf

[K. Harkay, Z. Huang, E. Lessner, and B. Yang, Proc. PAC 2001, 1915]

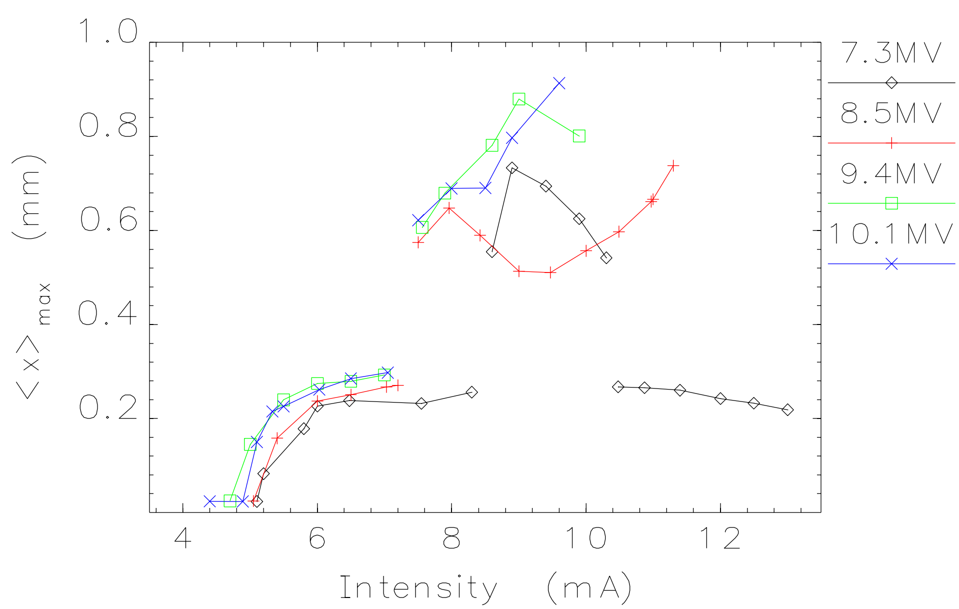

Dual-sweep streak camera image of single bunch undergoing coherent horizontal oscillations in bursting mode: bunch does not completely decohere

[data courtesy of B. Yang; K. Harkay et al., Proc of 1999 PAC, 1644]

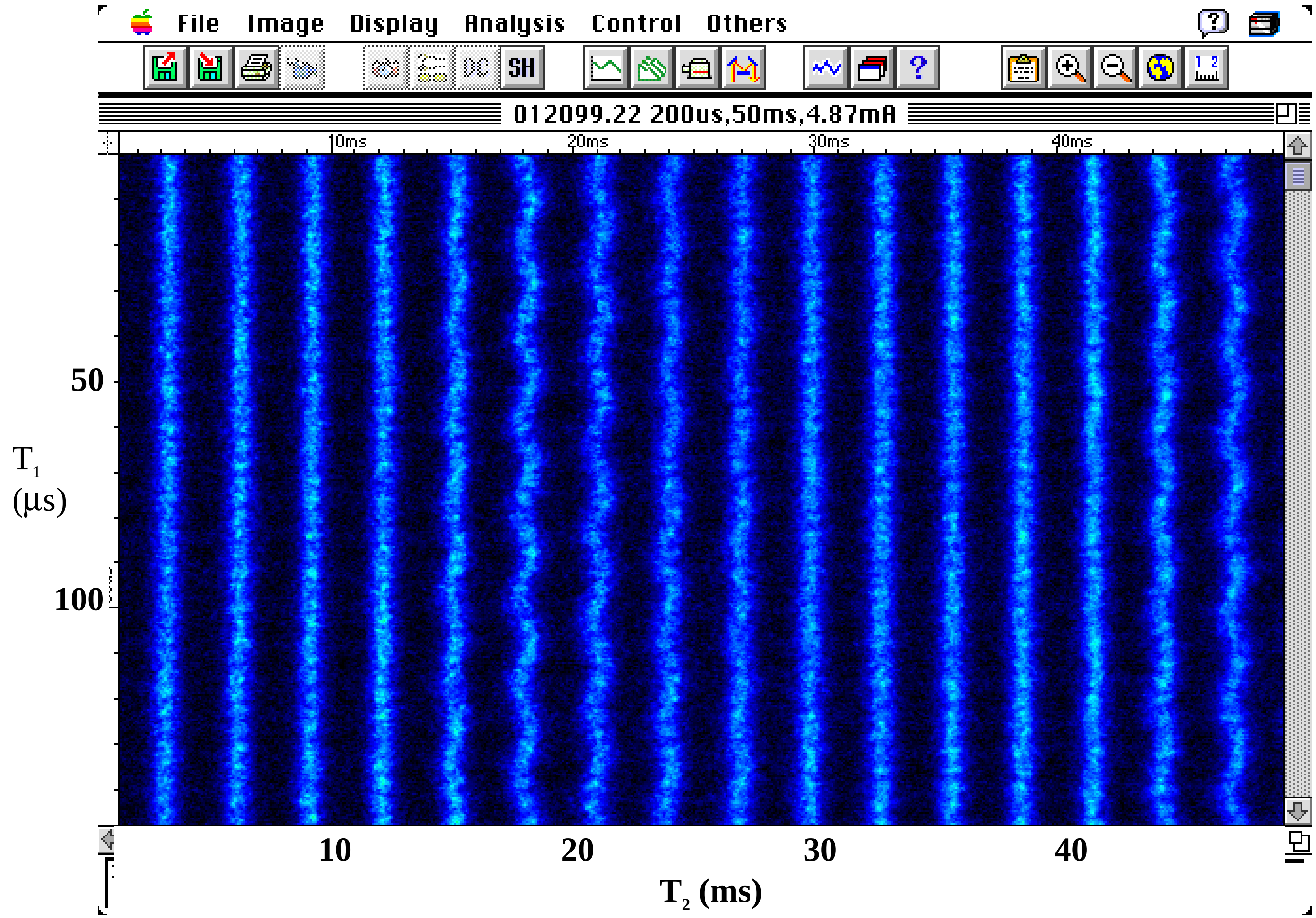

Measured bunch lengthening vs V_{rf}

(L. Emery, M. Borland, A. Lumpkin; no 5-mm ID chambers)

$Z_{||}/n \approx 0.5\ \Omega$ (estimated) [Y.-C. Chae et al., Proc. of 2001 PAC, 1817]

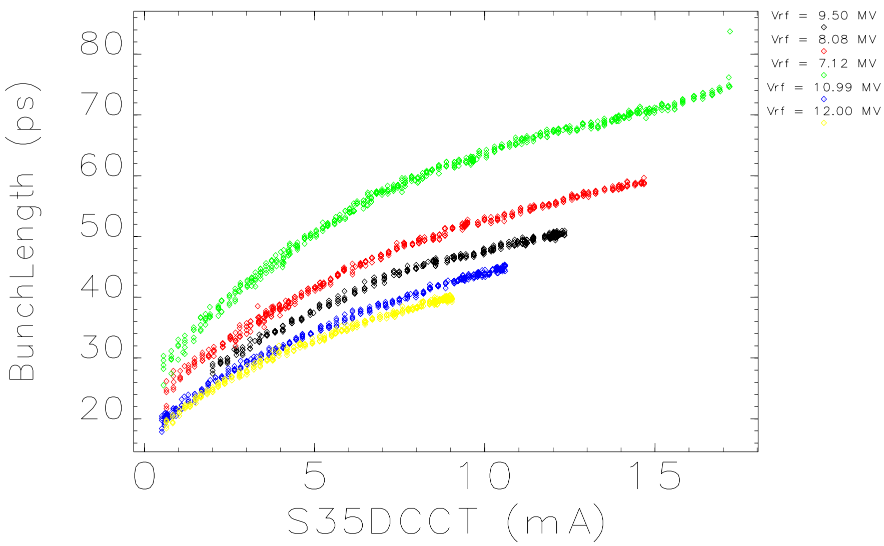

Measured δ and ε_x vs I_b (V_{rf} 7 MV, nominal $\xi_{x,y}$)

[K. Harkay, Z. Huang, E. Lessner, and B. Yang, Proc. PAC 2001, 1915]

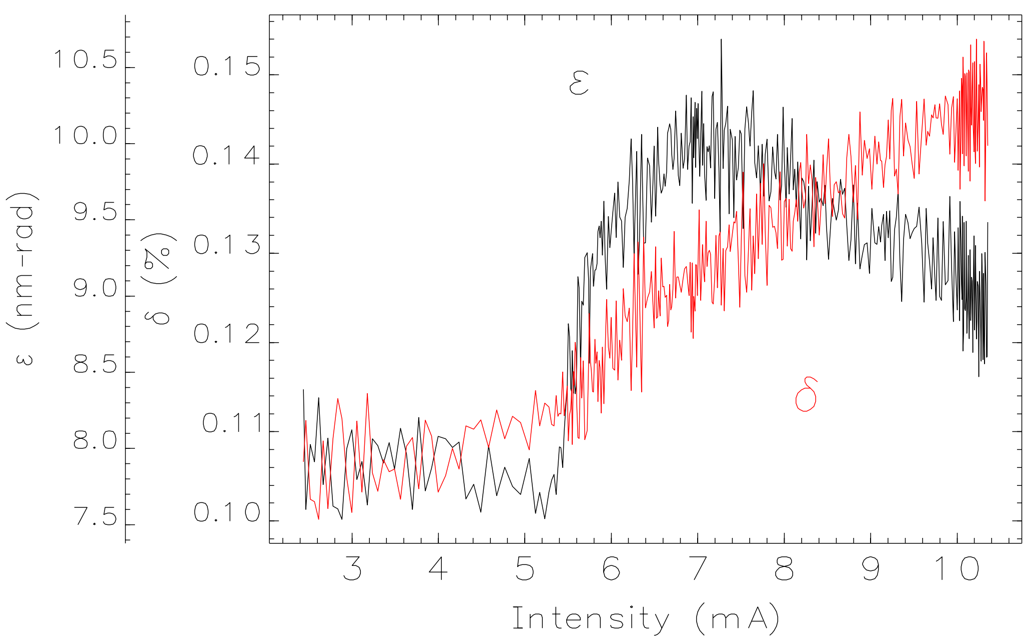

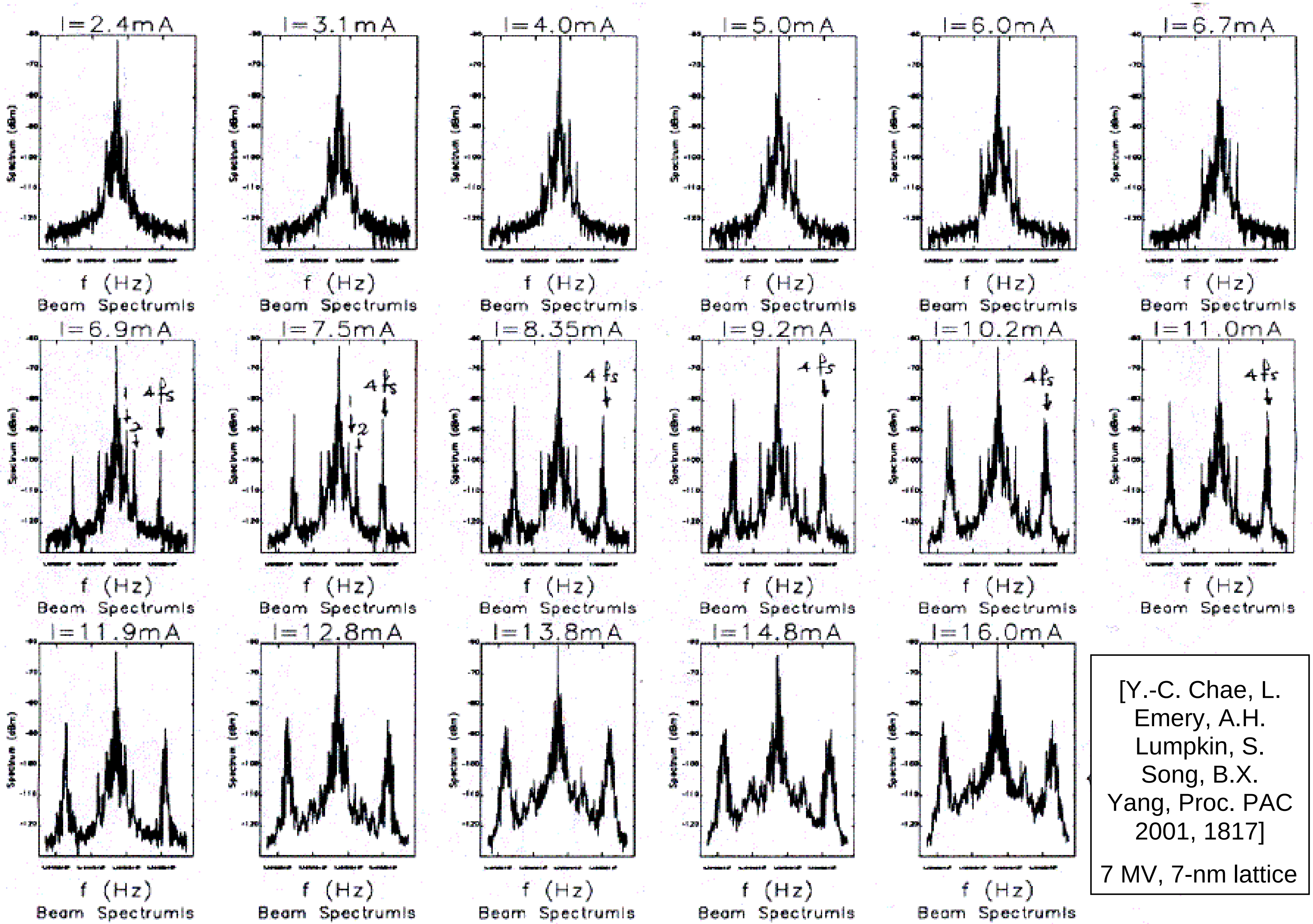

[Y.-C. Chae, L. Emery, A.H. Lumpkin, S. Song, B.X. Yang, Proc. PAC 2001, 1817]

7 MV, 7-nm lattice

Main Sources of Impedance in the SR

Single-bunch instabilities

- small-gap ID chambers
    - resistive wall impedance
    - geometric impedance (transitions)
- other discontinuities: rf fingers, kickers, scraper “cavity”
- “trapped” chamber modes?

Multibunch instabilities

- rf cavity higher-order modes
- other discontinuities: scraper “cavity”
- “trapped” chamber modes?

APS Storage Ring chambers

Standard

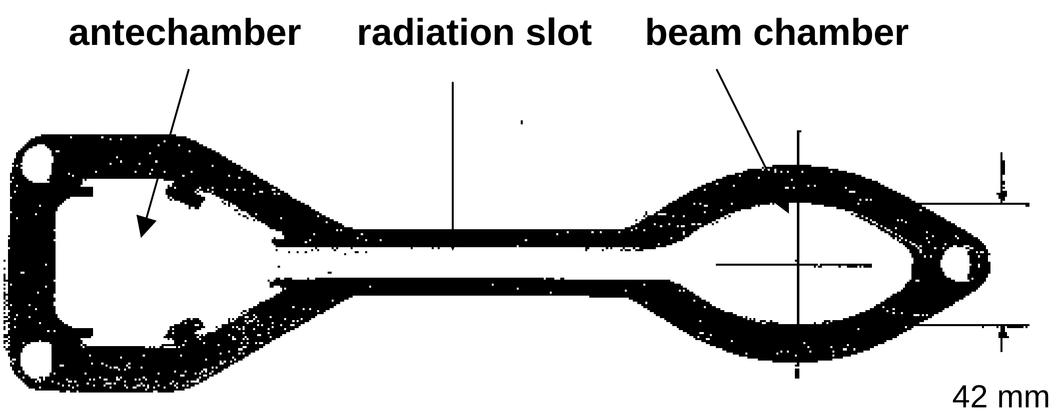

8-mm gap ID chamber

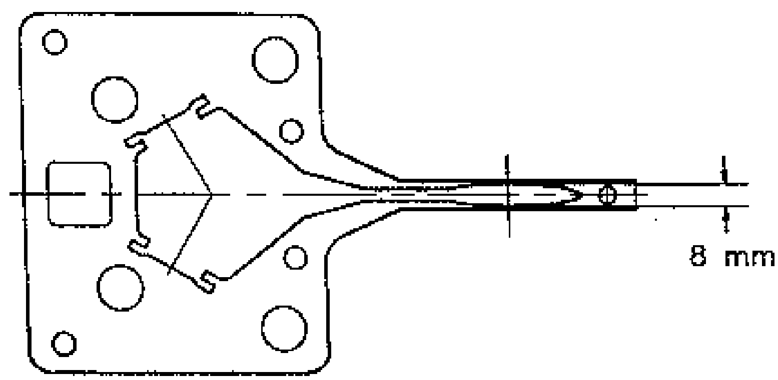

5-mm gap ID chamber

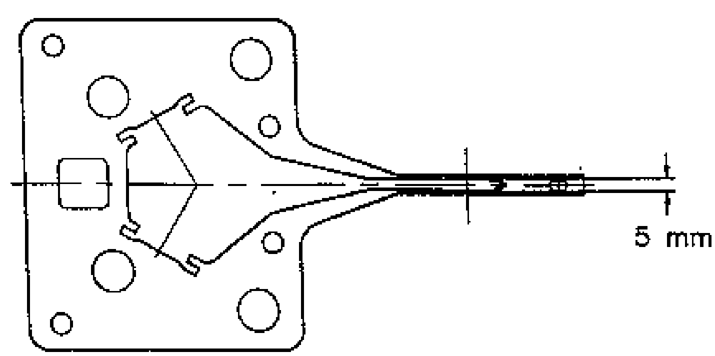

ID chamber transitions

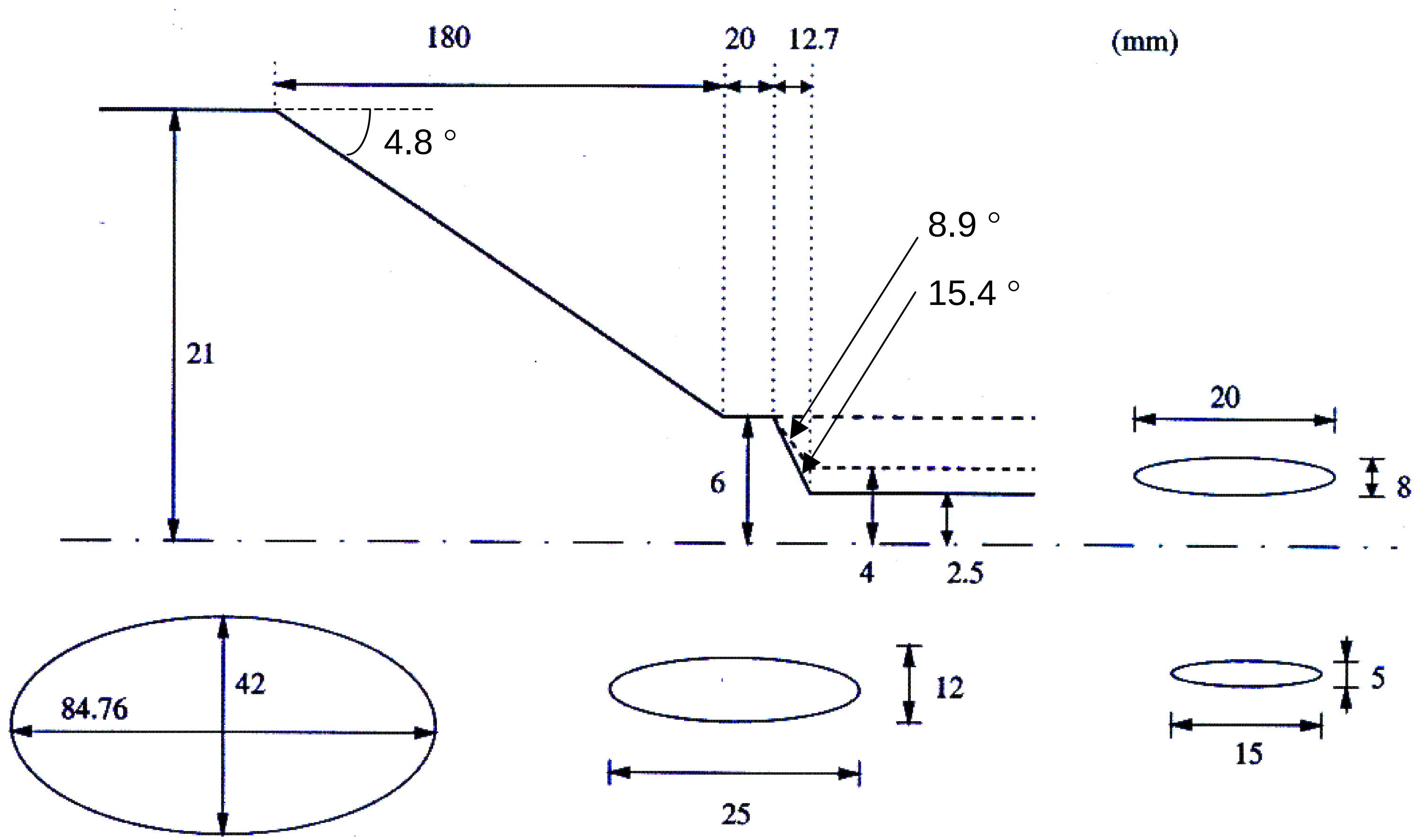

[Fig. courtesy of S.-B. Song, formerly at APS (post-doc), unpublished]

Impedance and Instabilities Plan

- Machine impedance database (Chae et al.)
  - MAFIA calculations ($Z_{x,y}$, PAC01 – Z_z)
  - Local tune shift using lattice model(V. Sajaev, C.-X. Wang – $Z_{x,y}$)
  - Local bump method (PAC01 – Z_y)
- Characterize longitudinal instability experimentally – validate $Z_{||}$
  - Apply $Z_{||}$ calculated from MAFIA to model with *elegant* code to reproduce bunch lengthening, $\Delta\sigma_t/\Delta I$, and microwave instability, $\Delta\delta/\Delta I$
- Characterize transverse instability experimentally – validate $Z_{\perp}$
  - Instability threshold, growth rate, and saturation amplitude vs V_{rf}, ξ, $\Delta\nu_x/N_x^2$, dispersion
- Instability photon diagnostics
  - Details of decoherence over bursts
- Other supporting studies
  - Nonlinear dynamics
  - Measure frequency spectrum evolution to look for mode-coupling and/or parametric resonance signatures

Impedance Database

- Goal

Wakepotential (APS Storage Ring) =

20*(8-mm ID Chamber) + 2*(5-mm ID Chamber) +

400*(BPM) + 80*(C2 Crotch Absorber) +
……..

- Standardize Wakepotential

1. Data in SDDS format
   - S, Wx, Wy, Wz

2. Uniform simulation conditions
   rms bunch length ➔ SIGz = 5 mm,
   mesh size ➔ dz = 0.5 mm,
   wakelength ➔ SBT = 0.3 m

3. Deposit the authorized wakepotentials in
   ~aps/ImpedanceDatabase/SR
   ➔ Available to everyone to read files

Y.-C. Chae

Impedance Database (cont.)

Vacuum Chamber Components

- Old components (experience)

  - Insertion Device Chambers
  - RF Cavities + Transition
  - Crotch Absorbers
  - Horizontal/Vertical Scrapers
  - Septum Intrusion
  - Stripline Monitors …….

- New components

  - BPMs
  - SR absorber between rf cavities
  - Vacuum port (slotted rf screen)
  - Shielded bellow

Y.-C. Chae

Impedance Database (cont.)

Example: Insertion Device Chambers

- Insertion Device Chambers
  - 5-mm-gap chamber
  - 8-mm-gap chamber
  - 12-mm-gap chamber

- Steps taken for 3-D Wakepotential

I. 2-D ABCI calculation for circular chamber (High confidence)
II. 2-D ABCI vs. 3-D MAFIA for circular pipe (Compare)
III. 3-D MAFIA for elliptical chamber (Final result)

Y.-C. Chae

Impedance Database (cont.)

2-D ABCI vs. 3-D MAFIA (Compare)

Geometry

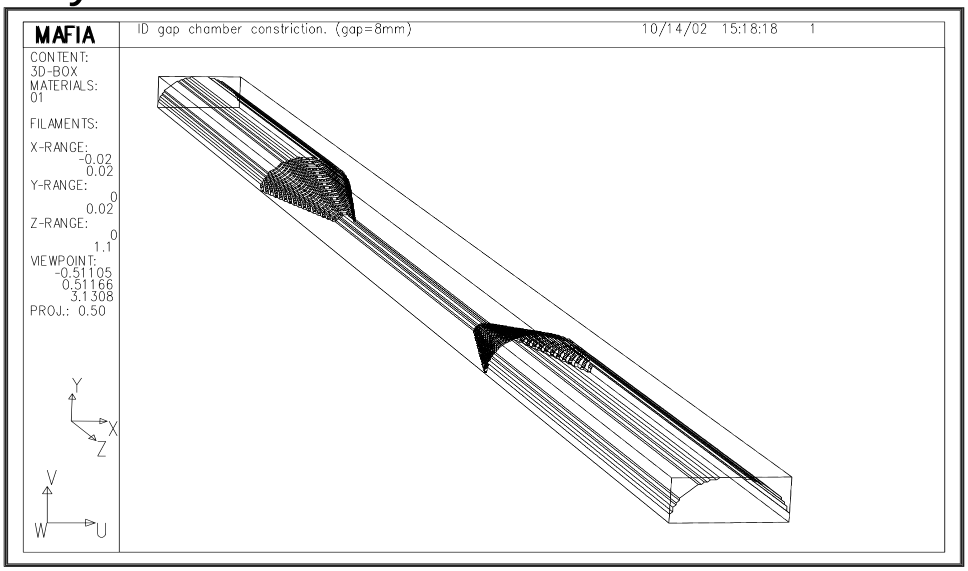

Results

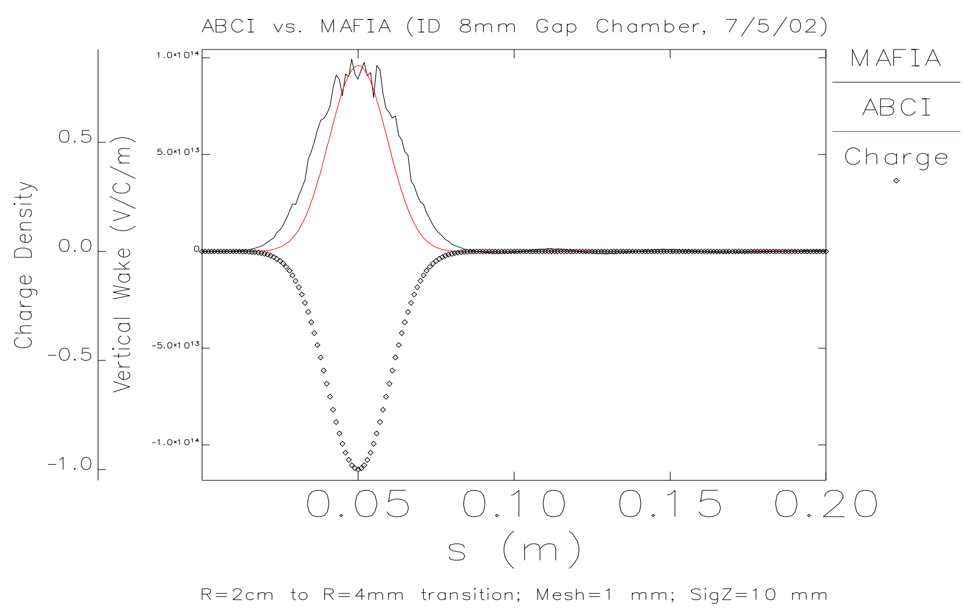

Y.-C. Chae

Impedance Database (cont.)

3-D MAFIA Results for Elliptical ID Chamber (Wakepotential & Impedance)

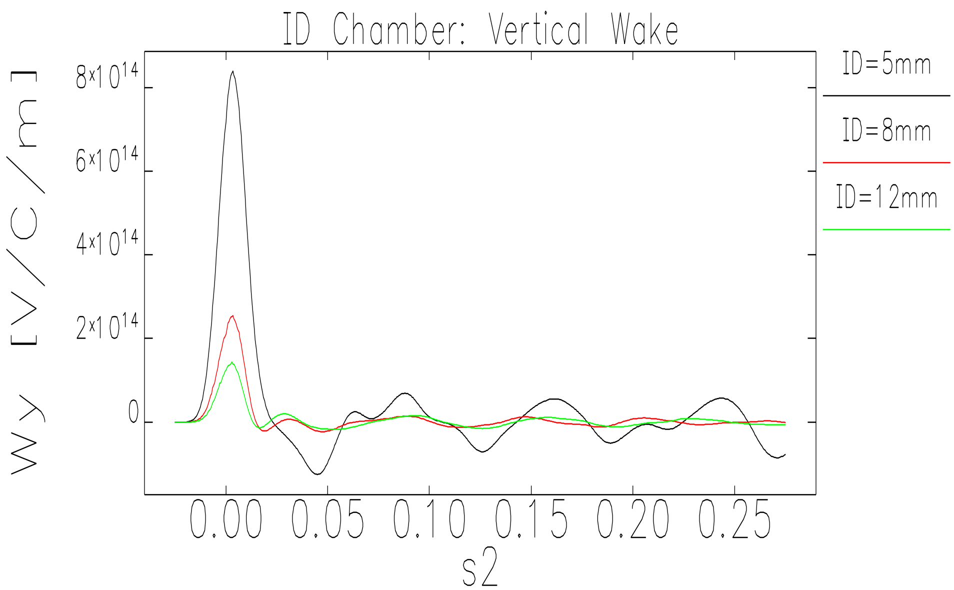

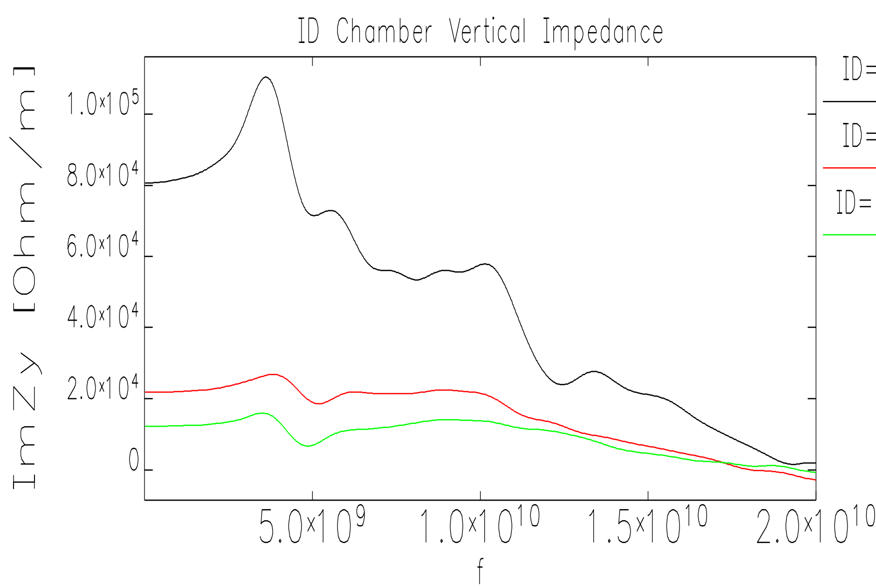

Y.-C. Chae

8-mm-gap ID vacuum chamber impedance

Z_y (effective) estimated five ways:

1. $Z_y = (Z_{RW} + Z_{geom})$ determined experimentally from change in tune slope, $\Delta\nu/\Delta I$, as a function of no. of chambers [N. Sereno et al, Proc. of 1997 PAC, 1700]:

Z_y = 53 kΩ/m per chamber x 20 = 1.1 MΩ/m

---

2. Simulations with Z_y represented by broad-band resonator impedance model reproduced measured tune slope and intensity threshold for TMCI at low chromaticity [K. Harkay et al, Proc. of 1999 PAC, 1644]:

exp:	$\Delta\nu_x/\Delta I = -8\times10^{-4}$/mA	$\Delta\nu_y/\Delta I = -2.6\times10^{-3}$/mA
model:	**0.2 MΩ/m**	**1.2 MΩ/m**
I_{TMCI} thresh:	**4.4 mA**	**2.2 mA**

---

3. Impedance calculated: resistive wall and geometric

a. resistive wall ∝ 1/b³

$$\frac{Z_{1_{x,y}}^{\perp}}{L} = \frac{c}{\omega}\frac{1+\mathrm{sgn}(\omega)\,j}{\pi b^3\delta\sigma}G_{1_{x,y}} \quad\Rightarrow\quad Z_{1_{x,y}}^{\perp}\left[\frac{\mathrm{k\Omega}}{\mathrm{m}}\right] = \left(1+\mathrm{sgn}(\omega)\,j\right)\frac{25500}{b[\mathrm{mm}]^3\sqrt{f\,[\mathrm{MHz}]}}G_{1_{x,y}}$$

f = cutoff frequency = c/2πb = 13 GHz

G_{1y} = 0.825 [Gluckstern and van Zeijts, CERN SL/AP 92-25, Jun 1992]

Z_{RW} (per 8-mm chamber, L = 5 m) = **3.4 kΩ/m**

b. geometric (transition): assuming a perfectly conducting circularly cylindrical tube of half-height b=4 mm, angle θ [Bane and Krinsky, Proc. of 1993 PAC, 3375]

$$W_\perp = \frac{Z_0 c}{\pi b}\left(\frac{2\theta}{\pi}\right)^{1/2} \frac{1}{\sqrt{2\pi}\sigma_s} \exp\left(\frac{-s^2}{2\sigma_s^2}\right) = 4 \times 10^{14}\ \Omega\text{/m-s per transition}$$

$Z_\theta = 2 \times (\sigma_s/c) W_\perp = 26$ kΩ/m (5-mm: $Z_\theta = 55$ kΩ/m)

$Z_\theta = 20 \times 26 = 0.5$ MΩ/m

c. totals

8-mm chamber: $Z_y = Z_{RW} + Z_\theta = 3.4 + 26 = 30$ kΩ/m

5-mm chamber: $Z_y = Z_{RW} + Z_\theta = 12 + (2.1 \times 26) = 70$ kΩ/m

---

4. MAFIA calculations of wake potentials: Z_θ from extracted tune slopes for geometric component (Y.-C. Chae)

8-mm ID: 20 kΩ/m

5-mm ID: 80 kΩ/m

---

5. Local bump method Z_y measurements [L. Emery, G. Decker, J. Galayda, Proc. of 2001 PAC, 1823]

8-mm: Z_y = 16 kΩ/m

5-mm: Z_y [kΩ/m] = 96 ± 8 kΩ/m (ID3); 78 ± 14 kΩ/m (ID4)

---

6. Local betatron phase shift [V. Sajaev and C.-X. Wang]

Work in progress: prelim. results agree with methods 4 & 5

Related R&D

- AP Group is developing tools to characterize lattice
    - Response matrix fit (V. Sajaev)
    - Model-independent analysis (C-X. Wang)
- Beta function correction and betatron phase advance
    - Lower sextupole strength for chromaticity correction
    - Local impedance

Increasing brightness of x-rays

- Brightness is the main single parameter characterizing a synchrotron light source. It is inversely proportional to the electron beam emittance.
- Over the last one and a half years, APS has made two big steps toward increasing the brightness:

Lattice: "High emittance" 7.7 nm×rad	→	Lattice: "Low emittance" 3.3 nm×rad 11/7/2001	→	Lattice: "Lower emittance" 2.4 nm×rad 10/15/2002

Response matrix fit allowed us to perform these changes quickly and ensured that the delivered beam parameters corresponded to the designed ones.

V. Sajaev

Orbit response matrix fit

- The orbit response matrix is the change in the orbit at the BPMs as a function of changes in steering magnets

$$\begin{pmatrix} x \\ y \end{pmatrix} = M_{\substack{measured \\ model}} \begin{pmatrix} \theta_x \\ \theta_x \end{pmatrix}$$

- The response matrix is defined by the linear lattice of the machine; therefore it can be used to calibrate the linear optics in a storage ring.
- Modern storage rings have a large number of steering magnets and precise BPMs, so measurement of the response matrix provides a very large array of precisely measured data.

Exploitation of the model

- Improving the performance of the existing machine
  - Beta function correction – to improve lifetime, injection efficiency and to provide users with the radiation exactly as specified
  - BPM gain calibration
- Creation of new lattices
  - Increasing brightness of x-rays by decreasing the beam emittance
  - Exotic lattices:
    - Longitudinal injection to decrease beam motion during injection
    - Converging beta function to increase x-ray flux density

Model-Independent Analysis

- MIA is a statistical analysis (principal composition analysis) of spatial-temporal modes in beam centroid motion recorded by the BPMs
- Mostly independent of detailed machine models
- Inclusive rather than exclusive – various other data analysis methods such as Fourier analysis, map analysis, etc. (even machine modeling) are being incorporated
- Not a recipe for a specific measurement, but rather a paradigm that facilitates systematic measurements and analysis of beam dynamics

Advantage: High sensitivity, model-independent, noninvasive, systematic

Basic requirement: A large set of reliable turn-by-turn BPM histories

[Paper submitted to Phys. Rev.]

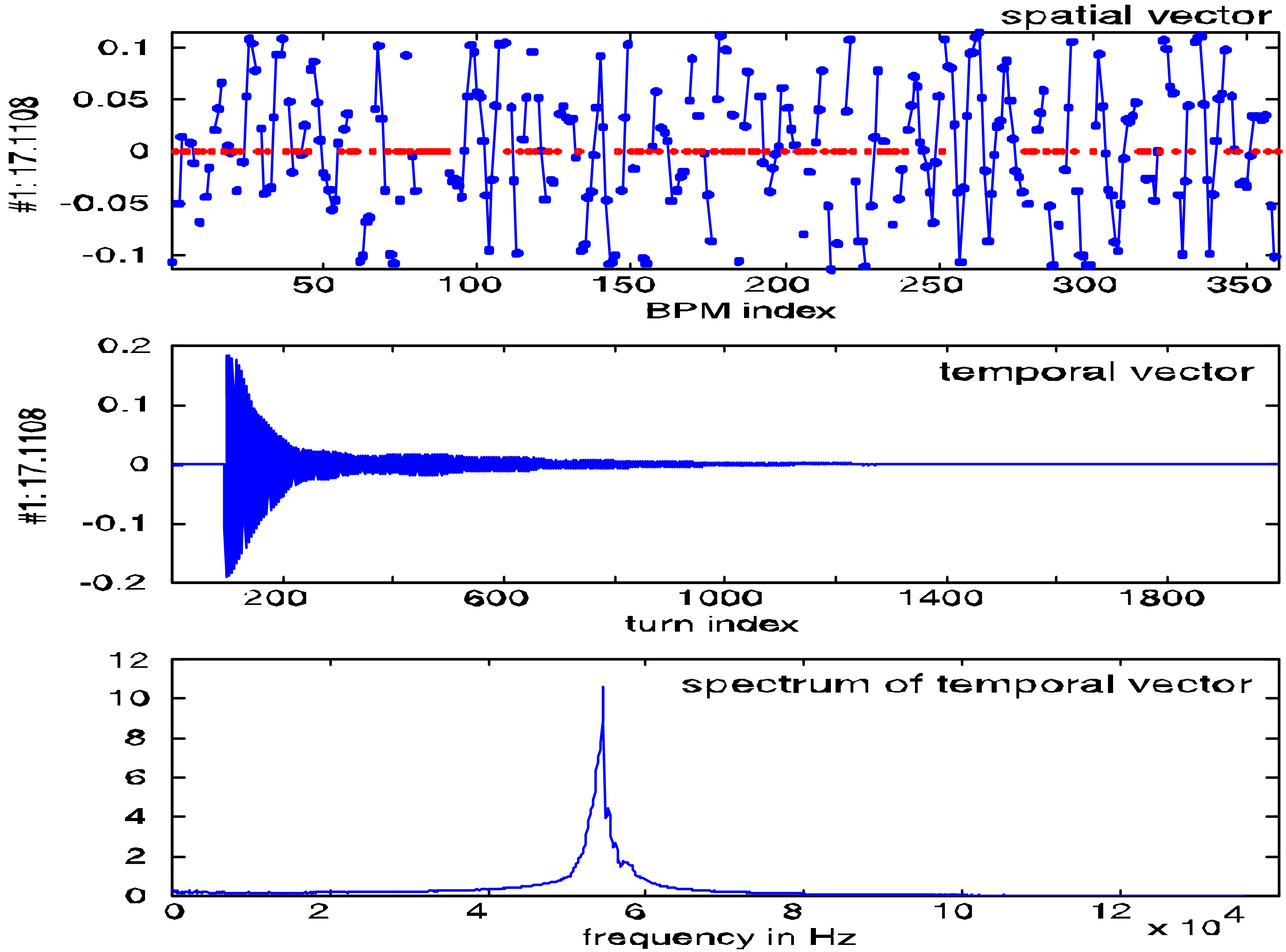
spatial vector
#1:17.1108
0.1
0.05
0
-0.05
-0.1
50
100
150
200
250
300
350
BPM index
temporal vector
0.2
0.1
0
-0.1
-0.2
200
600
1000
1400
1800
turn index
spectrum of temporal vector
12
10
8
6
4
2
0
2
4
6
8
10
12
x 10^4
frequency in Hz

C-X. Wang

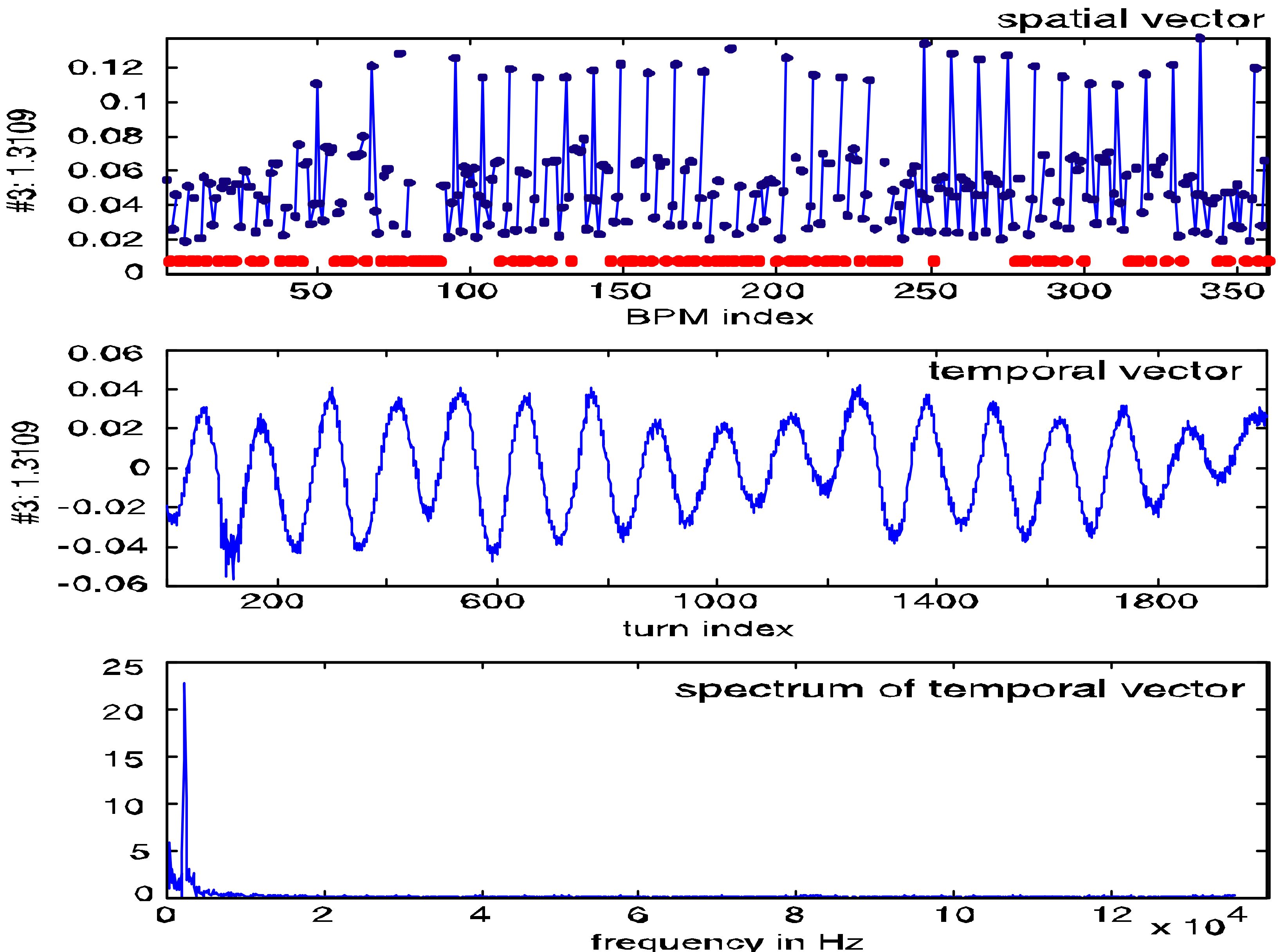
spatial vector
#3: 1.3109
0.12
0.1
0.08
0.06
0.04
0.02
0
50
100
150
200
250
300
350
BPM index
temporal vector
#3: 1.3109
0.06
0.04
0.02
0
-0.02
-0.04
-0.06
200
600
1000
1400
1800
turn index
spectrum of temporal vector
25
20
15
10
5
0
0
2
4
6
8
10
12
x 10^4
frequency in Hz

C-X. Wang

Phase changes due to a 0.5% quadrupole current change near 56th BPM

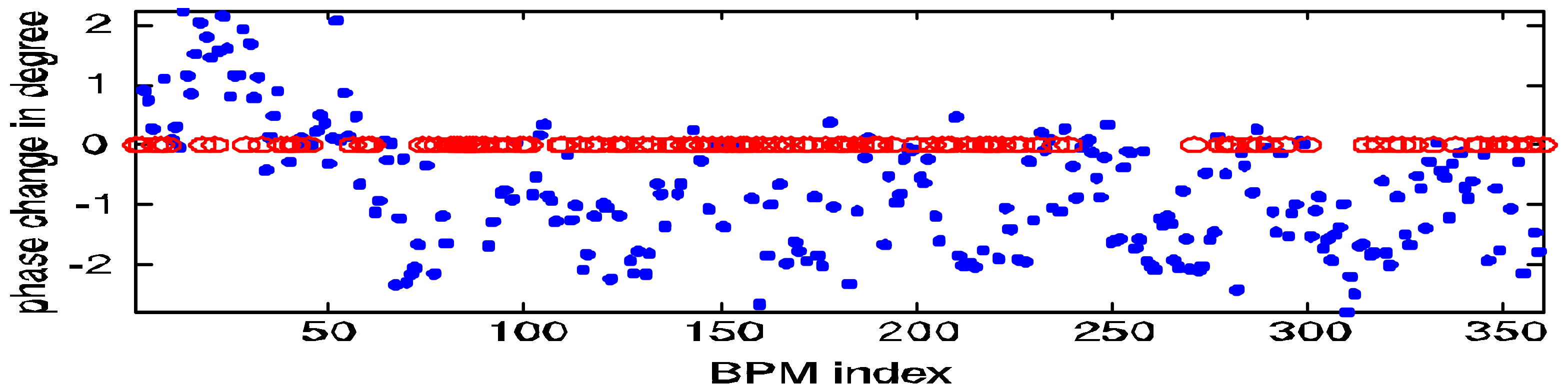

Phase changes due to a current-dependent wakefield (single bunch)

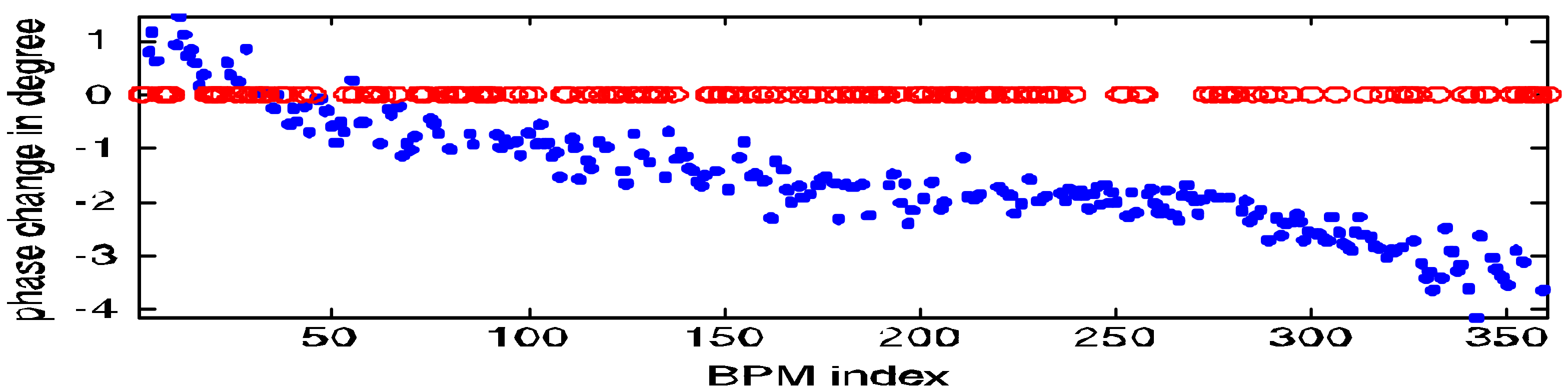

C-X. Wang

Other R&D topics (sample)

- Collaboration of Accelerator Research at Argonne (CARA) (Kwang-Je Kim)
    - APS
    - ATLAS (Rare Isotope Accelerator)
    - Advanced Wakefield Accelerator
    - Intense Pulsed Neutron Source
- Electron-cloud-induced multipacting resonance
- Ionization cooling
- Interleaved SR/FEL operation
- Injector development
- Ultrafast Thompson source, gamma source
- Frequency-Resolved Optical Gating (FROG) FEL analysis
- CSR microbunching at SURF
- Beam halos

The APS SASE FEL Schematic

The Low-Energy Undulator Test Line System

Present Configuration

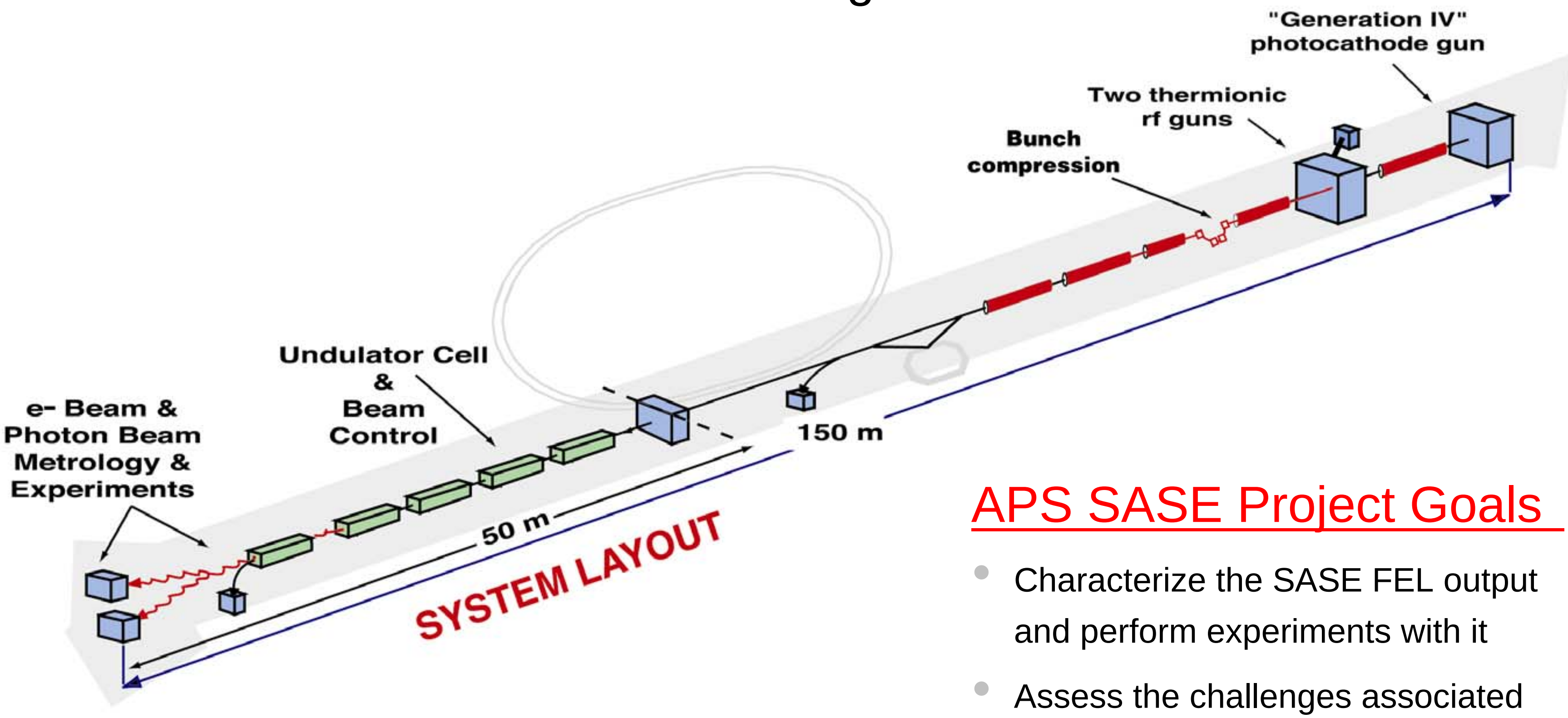

APS SASE Project Goals

- Characterize the SASE FEL output and perform experiments with it
- Assess the challenges associated with producing a SASE FEL in preparation for an x-ray regime machine

S. Milton

Basic Parameters for the APS FEL

PARAMETERS			
	Regime 1	Regime 2	Regime 3
Wavelength [nm]	530	120	51
Electron Energy [MeV]	217	457	700
Normalized rms Emittance (π mm-mrad)	5	3	3
Energy Spread [%]	0.1	0.1	0.1
Peak Current [A]	100	300	500
Undulator Period [mm]	33		
Magnetic Field [T]	1.0		
Undulator Gap [mm]	9.3		
Cell Length [m]	2.73		
Gain Length [m]	0.81	0.72	1.2
Undulator Length [m]	5 x 2.4 then 9 x 2.4	9 x 2.4	10 x 2.4

S. Milton

The First APS FEL Experiment

Single Photon Ionization / Resonant Ionization to Threshold (SPIRIT)

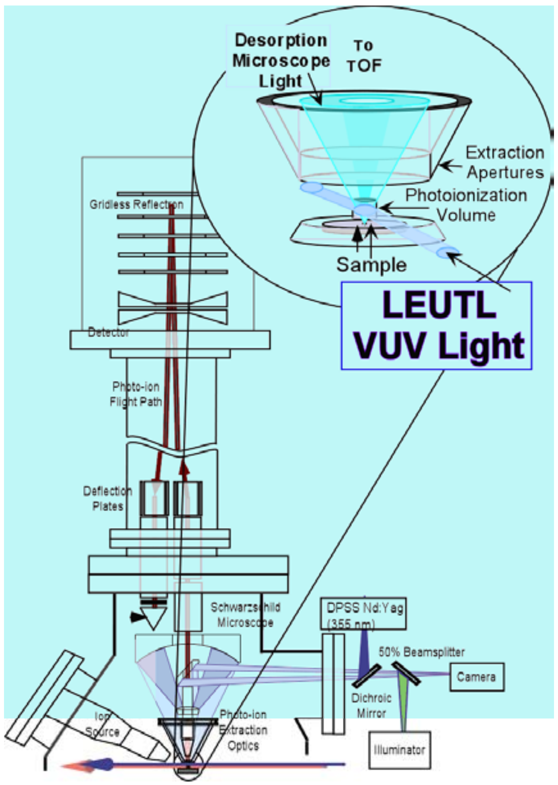

Coming 2002

M. Pellin MSD/ANL

SPIRIT will use the high VUV pulse energy from LEUTL to uniquely study –

- **Trace quantities of light elements**:
  H, C, N, O in semiconductors with
  100 times lower detection limit
- **Organic molecules <u>with minimal fragmentation</u>**
  - cell mapping by mass becomes feasible
    polymer surfaces
  - modified (carcinogenic) DNA
  - photoionization thresholds
- **Excited states of molecules**
  - cold wall desorption in accelerators
  - sputtering of clusters

J.W. Lewellen

Gun test stand status & future plans

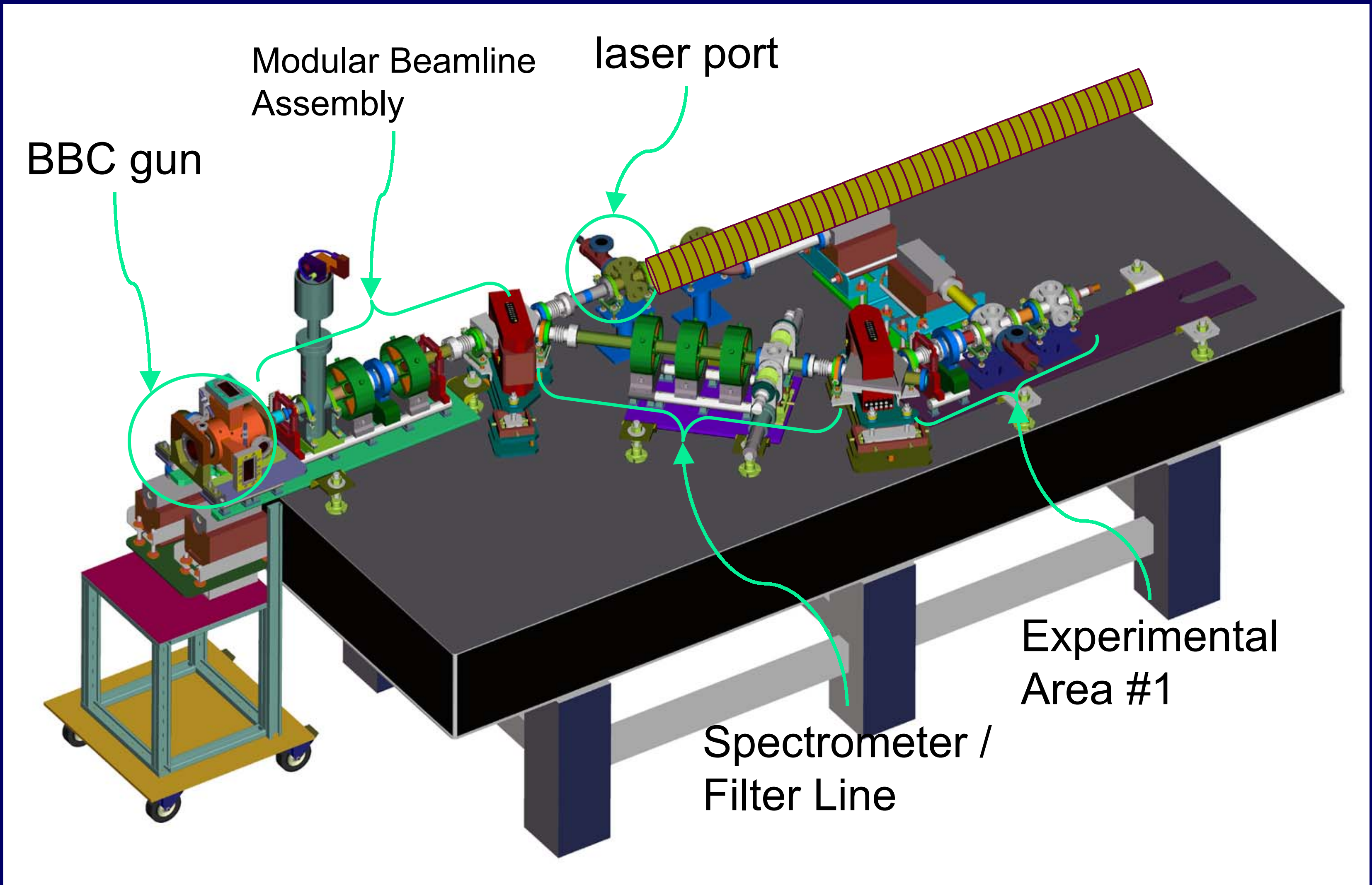

J.W. Lewellen

Higher-Order-Mode Gun High-Power Prototype Design

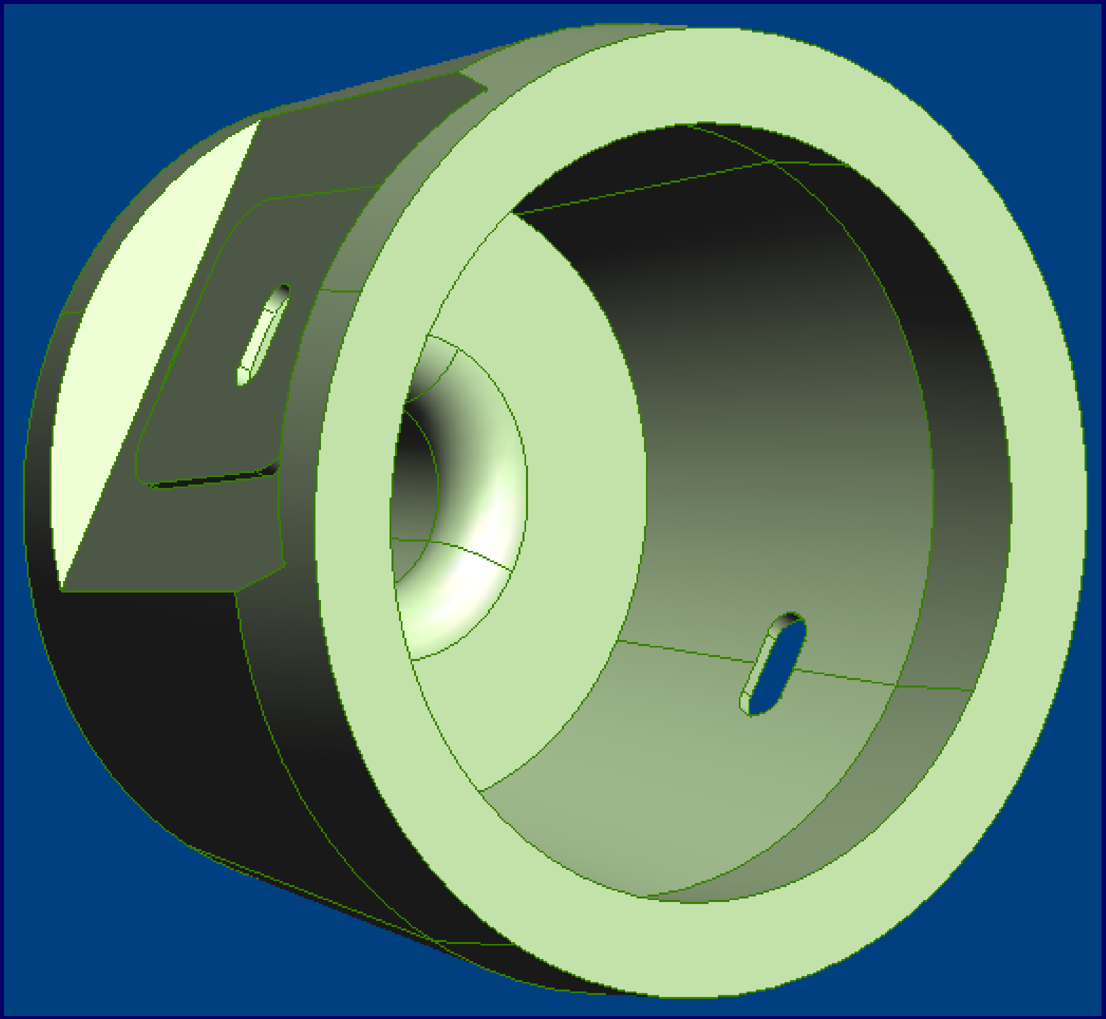

$TM_{0,1,1}$ Photoinjector Design

$TM_{0,1,1}$

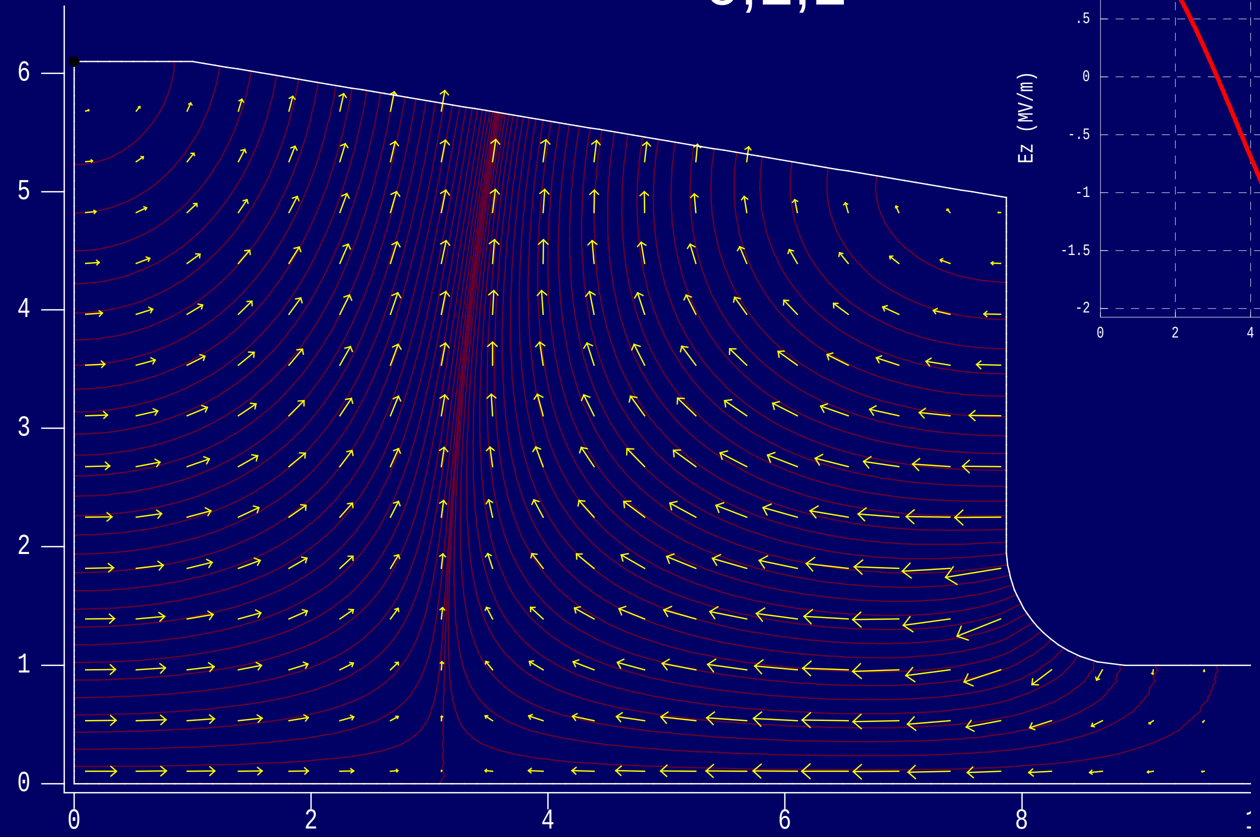

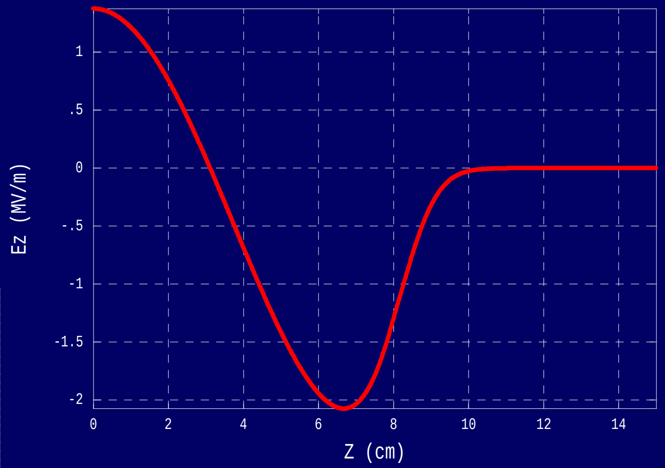

J.W. Lewellen

J.W. Lewellen

π-Mode Gun with Needle Cathode

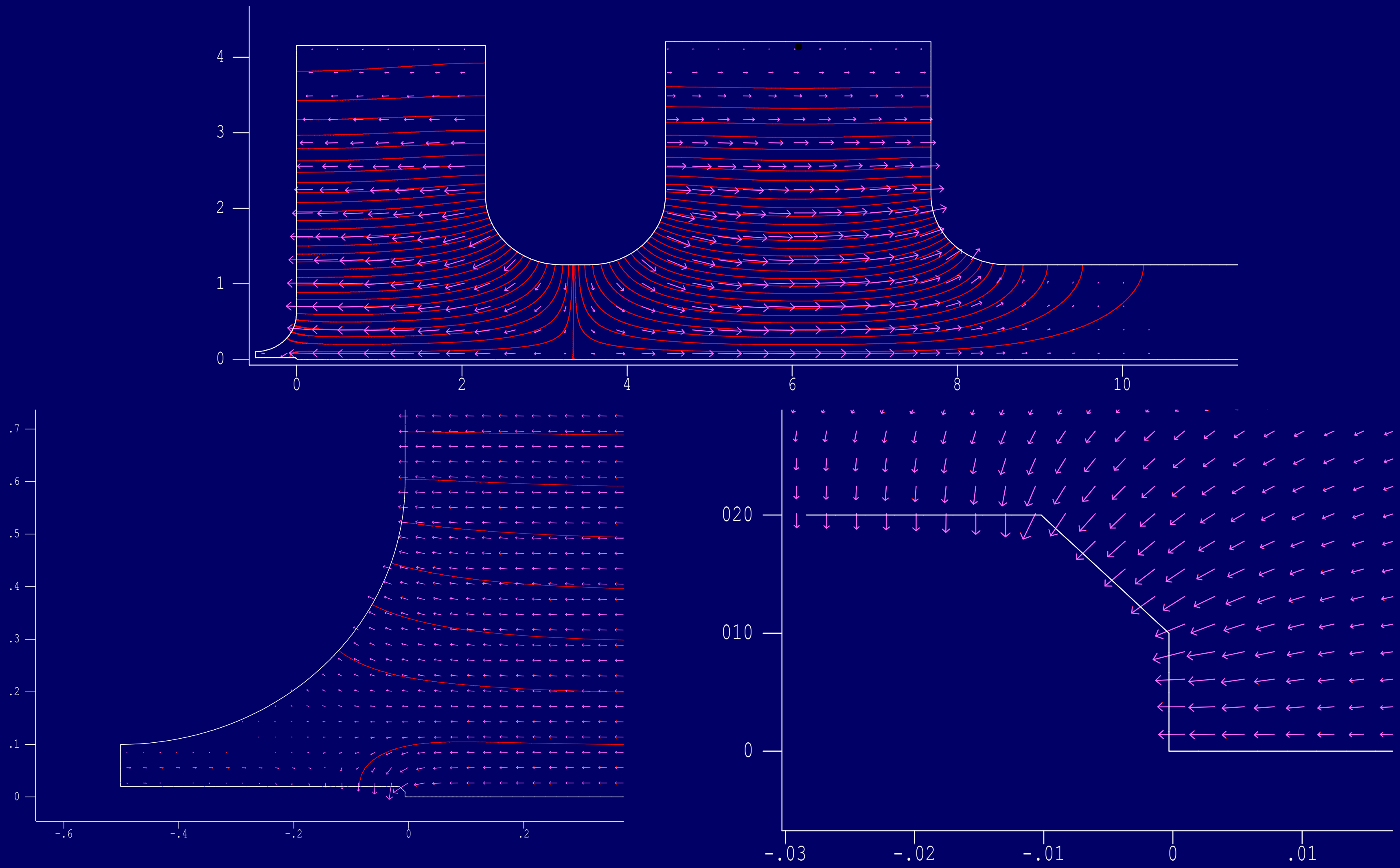

J.W. Lewellen

On-Axis Field Comparison

200-µm flat top radius, 300-µm needle radius

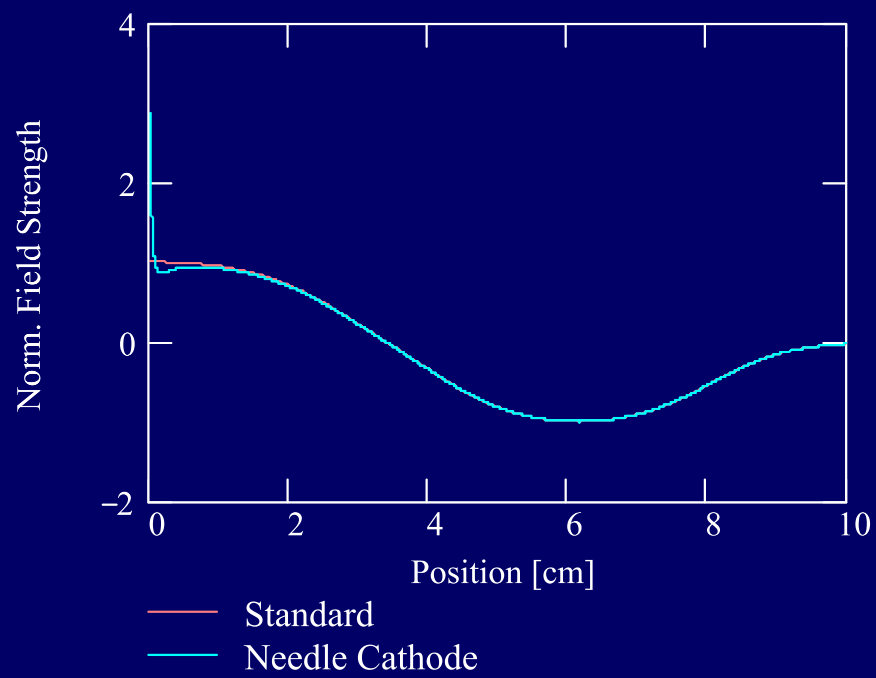

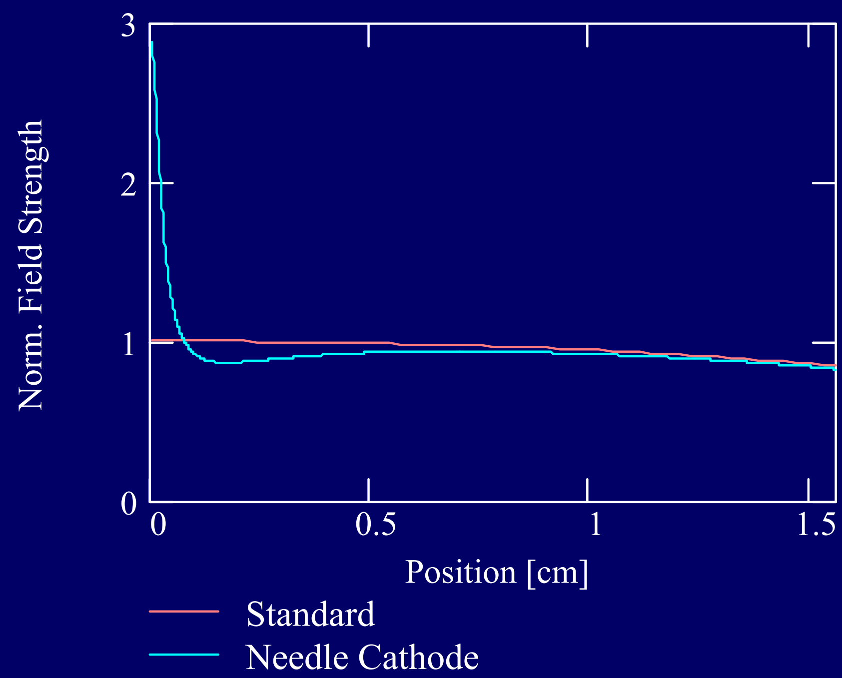

"Effective" needle height is ~ 1.3mm

Summary

- AP Group pursuing accelerator physics R&D in a number of areas
- Highest-priority topics address near-term anticipated User requirements

  e.g., characterize and mitigate single-bunch instability

- Also pursuing general accelerator physics topics for far-term light source development

  e.g., lattice characterization tools and source development